CrystEngComm

Accepted Manuscript

This article can be cited before page numbers have been issued, to do this please use: B. Barton, M. Adam and E. C. Hosten, *CrystEngComm*, 2026, DOI: 10.1039/D6CE00160B.

ROYAL SOCIETY OF CHEMISTRY

rsc.li/crystengcomm

View Article Online
DOI: 10.1039/D6CE00466B

The host potential of *N,N'*-bis(9-(4-methoxyphenyl)-9*H*-xanthen-9-yl)ethane-1,2-diamine for the xylene and ethylbenzene isomers, and its selectivity behaviour in mixed guest solutions

Benita Barton,* Muhammad-Ameen Adam and Eric C. Hosten

Department of Chemistry, Nelson Mandela University, PO Box 77000, Gqeberha (Port Elizabeth), 6031, South Africa.

Email: benita.barton@mandela.ac.za

Abstract

The crystallization of *N,N'*-bis(9-(4-methoxyphenyl)-9*H*-xanthen-9-yl)ethane-1,2-diamine (**H**) from each of the xylene and ethylbenzene isomers (*o*-Xy, *m*-Xy, *p*-Xy and EB) revealed that only the xylenes formed inclusion compounds with this host species, while EB was not included. The host:guest (H:G) ratios of the successfully formed complexes were 1:1, 1:1 and 1:2 for the *o*-Xy, *m*-Xy and *p*-Xy complexes, respectively. Guest solvents were also permitted to compete and crystallizations of **H** from such solutions revealed an unequivocal host selectivity in the order *o*-Xy > EB > *m*-Xy > *p*-Xy. Further binary guest competition experiments also demonstrated that this host species may serve as a purification tool, through host-guest chemistry protocols, of EB and *m*-Xy solvents that are tainted with small quantities of *o*-Xy and EB, correspondingly. Single crystal X-ray diffraction (SCXRD) analyses of the three single solvent complexes were employed in order to understand the host selectivity behaviour. The guest molecules in **H**·*o*-Xy and **H**·*m*-Xy (with guest solvents more preferred by **H** in the guest competition experiments) were accommodated in endless and unidirectional channels, and all of these guest species experienced (guest)C–H···π(host) stabilizing interactions with **H**. This was not the case for the guest species in **H**·2(*p*-Xy) (with the least favoured guest solvent). Here, two distinct types of guest molecules were observed, one being ordered and the other displaying positional disorder over two positions. Both of the latter disorder guest components were involved in this kind of interaction ((guest)C–H···π(host)) with **H**, while the ordered guest species appeared to be held in the complex through, predominantly, steric effects alone, and no (guest)C–H···π(host) or other close contacts were identified in this instance. This observation explained the distinct lack of selectivity of **H** for *p*-Xy relative to the remaining isomers in the guest competition experiments. Interestingly, the ordered and disordered guest molecules in this complex also occupied separate channel voids in the inclusion compound which were aligned along different axes in the unit cell. Finally, thermal analyses demonstrated that the three single solvent complexes in this investigation possessed comparable relative thermal stabilities as their guest release onset temperatures spanned a narrow range (T_{on} 39.2–41.7 °C).

Keywords

Selectivity; Supramolecular Chemistry; Crystallography; Purification; Ethylbenzene; Xylene

1. Introduction

The aromatic fraction of crude oil comprising *ortho*-xylene, *meta*-xylene, *para*-xylene and ethylbenzene (*o*-Xy, *m*-Xy, *p*-Xy and EB) are isomers (each with a molecular formula of C_8H_{10}) that possess near-identical physical properties, including boiling points, with a narrow boiling range of between 136 and 144 °C.[1,2] These compounds, therefore, distil over simultaneously when crude oil is heated.[3,4] Consequently, these mixtures are extremely challenging to separate into their components through fractional distillations, requiring excessive quantities of depleting fossil fuels, and resulting in intricate processes that are characterized by exorbitant costs.[5–7] However, efficient methods for their separation are imperative since each particular solvent is required in pure form for subsequent applications in the chemical industry. As examples, ethylbenzene is essential in order to produce styrene, a monomer with manifold applications in polymer science, including the production of plastics such as polystyrene.[8,9] *p*-Xylene, regarded as the more important of the four isomers, is necessary for the manufacture of polyethylene terephthalate, a ubiquitous polymer that largely fulfils the role of sterile food and drinks containers in outlets providing consumables to the public.[10–12] *o*-Xy and *m*-Xy are employed as starting materials towards phthalic anhydride and isophthalic acid, respectively, both of these intermediates also serving as monomers towards plastics and coatings.[13–17]

View Article Online
DOI: 10.1039/D6CE00160B

Owing to the importance of having processes that achieve these separations effectively that do not rely on the boiling points of these compounds, a number of different strategies have been investigated that have demonstrated some promise. These include extractive distillations, chromatography, inorganic membranes, zeolites, polymers, and metal-organic and hydrogen-bonded organic frameworks, to mention only a few.[18–24] However, despite the success of some of these separation protocols, many are not attractive, more especially with respect to scalability, recyclability and inflated costs.

Host-guest chemistry is an alternative separatory candidate that may be considered in order to effectively separate Xy/EB mixtures. This field of science relies on the selectivity of the "host compound" for one particular "guest species" when presented with a mixture of guest solvents.[25,26] In our own laboratories, this avenue for such separations has been extensively investigated with the view to discovering new host compounds with improved or different selectivities compared with those that are better known. The preferential behaviour of the host compound is dependent upon a number of factors, including the existence of noncovalent interactions in these complexes between host and guest (*e.g.*, π···π stacking, X–H···π close contacts, hydrogen bonding (classical and nonclassical) and van der Waals forces), steric influences as well as guest attributes (geometry, functional groups, *etc.*). To this end, host compounds derived from xanthone, thioxanthone, dibenzosuberone, dibenzosuberenone, tartaric acid and anthracene were designed, synthesized and investigated for their separation potential for mixtures of Xy/EB.[27–35] These host species more usually preferred *p*-Xy and/or *o*-Xy, while EB and/or the *meta* isomer remained largely disfavoured.

In the present work, an alternate host compound, *N*,*N*′-bis(9-(4-methoxyphenyl)-9*H*-xanthen-9-yl)ethane-1,2-diamine (**H**), was assessed for its host potential for each of the Xy/EB isomers through crystallization experiments (Figure 1). If host ability existed, **H** was then crystallized from various Xy/EB solutions in order to identify its preferential behaviour in these experimental conditions and to ascertain whether **H** may serve as a separatory or purification candidate for any of these mixtures. Additionally, all single solvent complexes were subjected to both SCXRD and thermal analyses to elucidate the mode of guest entrapment within the crystals of the complex as well as to determine the relative thermal stabilities of these complexes. The present host compound has not been employed in this manner to date, and we report on the results so-obtained herein.

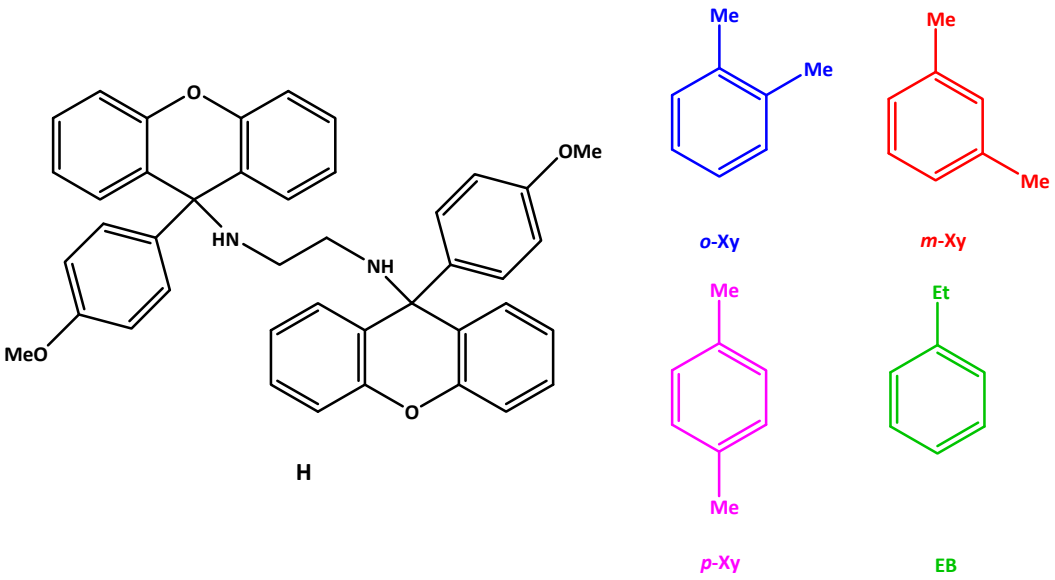

Figure 1 Structures of *N*,*N*′-bis(9-(4-methoxyphenyl)-9*H*-xanthen-9-yl)ethane-1,2-diamine (**H**), and the potential guest solvents *o*-xylene, *m*-xylene, *p*-xylene and ethylbenzene (*o*-Xy, *m*-Xy, *p*-Xy and EB).

2. Experimental

2.1 General

View Article Online
DOI: 10.1039/D6CE00160B

N,*N'*-Bis(9-(4-methoxyphenyl)-9*H*-xanthen-9-yl)ethane-1,2-diamine (**H**) was prepared from xanthone using chemicals that were procured from Merck (South Africa). The EB and Xy solvents were also obtained in this manner, and these were used as received.

All ^{1}H-NMR experiments were conducted by means of a Bruker Ultrashield Plus 400 MHz spectrometer with $CDCl_3$ as the deuterated solvent. Topspin 4.4.1 software was employed for spectral data analysis.

The SCXRD experiments for the crystal structures of guest-free **H**, **H**·*o*-Xy, **H**·*m*-Xy and **H**·2(*p*-Xy) were performed at 200(2) K using a Bruker D8 Quest diffractometer with a Photon II CPAD detector and IμS 3.0 Mo source (Kα, λ = 0.71073 Å). APEX4[36] was used for data collection and SAINT[36] for cell refinement and data reduction. Data were corrected for absorption effects using the multi-scan method implemented in SADABS.[37] The structure was solved using SHELXT–2018/2[38] using a dual-space algorithm and refined by least-squares procedures using SHELXL-2025/1[39] with SHELXLE[40] as a graphical interface. Diagrams were drawn with ORTEP-3 for Windows version 2023.1 (Supplementary Information (SI)).[41] All non-hydrogen atoms were refined anisotropically. Carbon-bound H atoms were placed in calculated positions (C–H bond lengths of 0.95 Å for aromatic carbon atoms, 1.00 Å for methine, 0.99 Å for methylene) and were included in the refinement in the riding model approximation, with U_{iso}(H) set to 1.2U_{eq}(C). When possible the H atoms of the methyl groups were allowed to rotate with a fixed angle around the C–C bond to best fit the experimental electron density (HFIX 137 in the SHELXL program[39]) with U_{iso}(H) set to 1.5U_{eq}(C) and C–H bond lengths of 0.98 Å; otherwise they were placed in calculated positions.

The nitrogen-bound hydrogens were located on a difference map and, when possible, allowed to refine freely. The crystal structures of guest-free **H**, **H**·*o*-Xy, **H**·*m*-Xy and **H**·2(*p*-Xy) were deposited at the Cambridge Crystallographic Data Centre and their respective CCDC numbers are 2530251–2530254.

GC-MS analyses were carried out using an Agilent 7890A GC equipped with an Agilent J&W Cyclosil-B column coupled to a flame ionization detector. The method involved an initial 1 min hold time at 50 °C. A ramp rate of 10 °C·min^{-1} was then implemented until a final temperature of 90 °C was reached, and this temperature was maintained for 3 min. The flow rate was 1.5 mL·min^{-1} and the split ratio 1:40.

A Perkin Elmer STA 600 module system was employed for the thermal experiments; here, data were analysed by means of Pyris software. Samples were placed in ceramic pans with nitrogen serving as the purge gas. The heating rate was 10 °C·min^{-1} and the temperature range employed was from approximately 40 to 350 °C.

2.2 Synthesis of *N*,*N'*-bis(9-(4-methoxyphenyl)-9*H*-xanthen-9-yl)ethane-1,2-diamine (H)

The host compound was prepared from xanthone by considering the synthetic procedures in a previous report.[42]

2.3 Independent host crystallization experiments from each of the xylenes and EB

In order to determine whether **H** has the ability to include Xy/EB, the host compound was crystallized independently from each of these liquids. As such, **H** (0.05 g, 0.08 mmol) was dissolved in an excess of the guest in a glass vial, with mild heat being applied to ensure complete host dissolution. The vial was left open at ambient temperature and pressure to allow evaporation of some of the liquid to occur which, in turn, induced crystallization. The crystals were isolated by means of vacuum filtration and washed with low boiling petroleum ether whilst still under suction. Analysis was then through ^{1}H-NMR experiments to confirm whether inclusion had been successful and then to calculate the host:guest (H:G) ratios by comparing the integrals of applicable host and guest resonance signals.

2.4 Host crystallization experiments from equimolar guest mixtures

In order to assess whether **H** possesses selectivity for a particular guest solvent, host crystallization experiments were conducted in mixed guest solutions that were prepared in equimolar proportions. All possible Xy/EB combinations were considered here. Thus, **H** (0.05 g, 0.08 mmol) was dissolved in the equimolar mixed guest solution (5 mmol combined amount), the vial lidded and sealed with parafilm and stored at ambient conditions. The resultant crystals were isolated and treated as

View Article Online
DOI: 10.1039/D6CE00160B

in the single solvent experiments. The guest ratios in any mixed complexes that formed in this manner were determined through GC analysis.

2.5 Host crystallization experiments from binary guest solutions with differing molar ratios

Subsequently, **H** was crystallized from binary guest solutions (G_A and G_B) in which the molar ratio of each guest present was varied (20:80, 40:60, 60:40 and 80:20 G_A:G_B). These crystallizations were carried out in an identical fashion to the aforementioned equimolar guest experiments. Analyses of the crystals were by means of GC, which provided the guest amounts in the so formed mixed guest complexes. Selectivity profiles were then constructed by plotting Z_A (or Z_B), the amount of G_A (or G_B) in the crystals, against X_A (or X_B), the amount of G_A (or G_B) in the original solution, according to the equation of Pivovar and colleagues, $K = Z_A/Z_B \times X_B/X_A$, where $X_A + X_B = 1$.[43] These plots provide a visual representation of the host selectivity behaviour in such varying guest proportions. K is the selectivity coefficient and may be calculated for each data point in these plots and serves as a measurement of the host selectivity. It has been reported that K values are required to be 10 or greater for effective separations of binary mixtures in a practical setting.[44] When K = 1, the host compound is not selective; this theoretical scenario is represented by the straight diagonal lines that have been inserted into each of these profiles for comparison.

2.6 Software

The crystal structures obtained from SCXRD analysis were analysed by means of program Mercury,[45] which was instrumental in preparing the unit cell, packing, noncovalent interaction and void diagrams. These latter figures required deletion of the guest molecules from the packing calculations and then analysing the spaces remaining using a probe with a 1.2 Å radius.

3. Results and discussion

3.1 Independent host crystallization experiments from each of the xylenes and EB

Table 1 summarises the results obtained when **H** was crystallized from each of the four isomers. Only EB was not enclathrated, while the H:G ratios of the three complexes that formed successfully were 1:1 (*o*-Xy and *m*-Xy) and 1:2 (*p*-Xy). (The applicable ^{1}H-NMR spectra for these complexes are provided in the SI).

Table 1 The H:G ratios of complexes of **H** when crystallized from each of the xylenes and EB.

Guest	H:G ratio
o-Xy	1:1
m-Xy	1:1
p-Xy	1:2
EB	[a]

[a]No inclusion occurred.

3.2 Host crystallization experiments from equimolar guest mixtures

Table 2 contains a summary of the results obtained after analysing the solids emanating from the equimolar solutions through GC. These experiments were conducted in duplicate to determine their replicability and, thus, the percentage estimated standard deviations (% e.s.d.s) are also provided in this table. Preferred guests are indicated in bold text for ease of analysis.

Table 2 Results from the equimolar mixed Xy/EB experiments.

o-Xy	*m*-Xy	*p*-Xy	EB	Guest ratio	% e.s.d.s
X	X			**59.9** : 40.1	1.4
X		X		**86.7** : 13.3	0.3
X			X	**80.7** : 19.3	0.8
	X	X		**53.5** : 46.5	0.7
	X		**X**	45.9 : **54.1**	2.5
		X	**X**	41.2 : **58.8**	0.3
X	X	X		**53.8** : 34.5 : 11.7	0.5: 0.2 : 0.3

X	X		X	**48.1** : 9.6 : 42.3	1.9 : 0.3 : 1.56
X		X	X	**66.6** : 12.8 : 20.6	2.5 : 2.3 : 0.2
	X	X	**X**	9.2 : 9.5 : **81.3**	0.6 : 0.3 : 0.9
X	X	X	X	**36.2** : 19.8 : 8.2 : 35.8	1.2 : 1.4 :0.2 : 2.4

A rapid scrutiny of the data contained in Table 2 suggests that **H** preferred *o*-Xy whenever it was present, followed by EB and then the *meta* isomer. Interestingly, *p*-Xy remained disfavoured in each instance. In more depth, the binary solutions involving *o*-Xy (*o*-Xy/*m*-Xy, *o*-Xy/*p*-Xy and *o*-Xy/EB) afforded crystals enriched in *o*-Xy, and between 59.9 and 86.7% of this isomer were measured in these mixed complexes. In the absence of *o*-Xy but presence of EB in these binary experiments (*m*-Xy/EB and *p*-Xy/EB), **H** selected more of EB (54.1 and 58.8%), while when both *o*-Xy and EB were not involved (*m*-Xy/*p*-Xy), the crystals contained an elevated quantity of the *meta* isomer (53.5%). These trends continued in the ternary experiments, and *o*-Xy remained favoured in the *o*-Xy/*m*-Xy/*p*-Xy, *o*-Xy/*m*-Xy/EB and *o*-Xy/*p*-Xy/EB solutions (53.8, 48.1 ang 66.6%, respectively), while in the absence of *o*-Xy (*m*-Xy/*p*-Xy/EB), more of EB (81.3%) was selected. Furthermore, and unsurprisingly, the quaternary solution also revealed an enhanced preference for *o*-Xy (36.2%). In summary, the host selectivity in these guest mixtures may thus be presented as in the order *o*-Xy > EB > *m*-Xy > *p*-Xy. These results are interesting given that, as mentioned earlier, many of the host compounds prepared in our laboratories more usually preferred *p*-Xy and/or *o*-Xy, while EB and/or the *meta* isomer were mostly disfavoured, and this is certainly not the case in the present investigation, with *p*-Xy being consistently the least favoured guest species.[27–35]

3.3 Host crystallization experiments from binary guest solutions with differing molar ratios

When two guest solvents were mixed in varying proportions, the selectivity profiles as displayed in Figures 2a–f were obtained after GC analysis on the solids emanating from the crystallization experiments.[43] Additionally, the K value for each data point contained in these plots are provided in Table 3; those values 10 or greater, where meaningful separations are plausible on a practical platform,[44] are provided in bold text.

a)

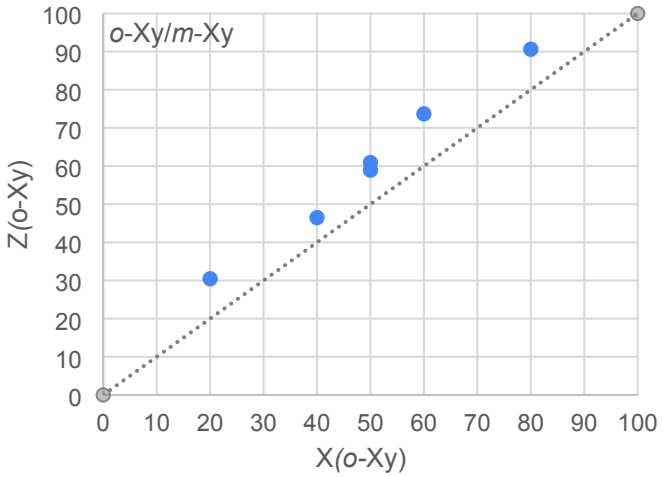

b)

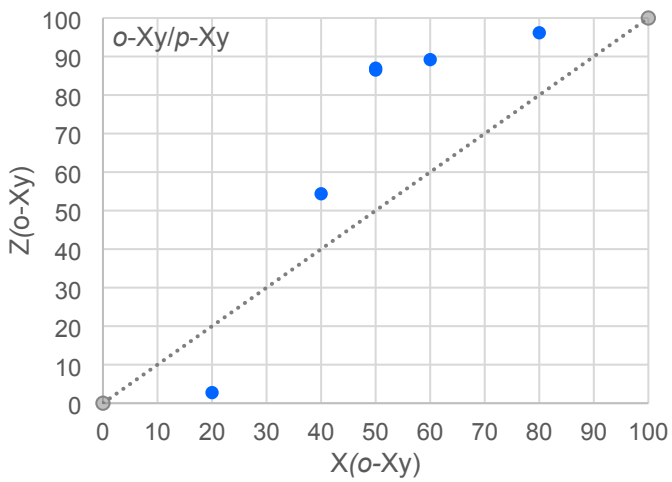

c)

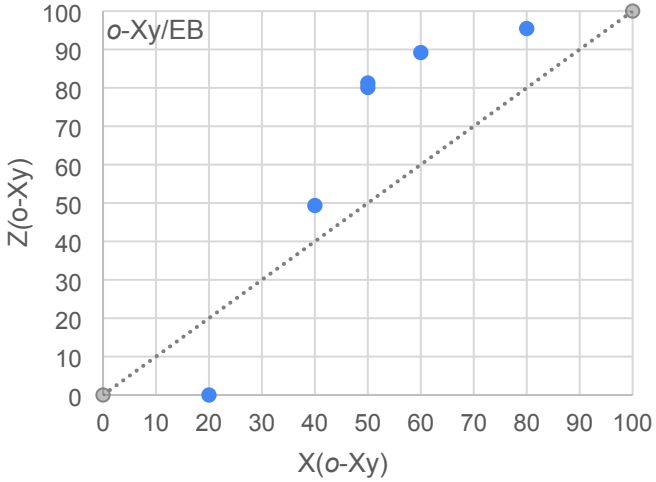

d)

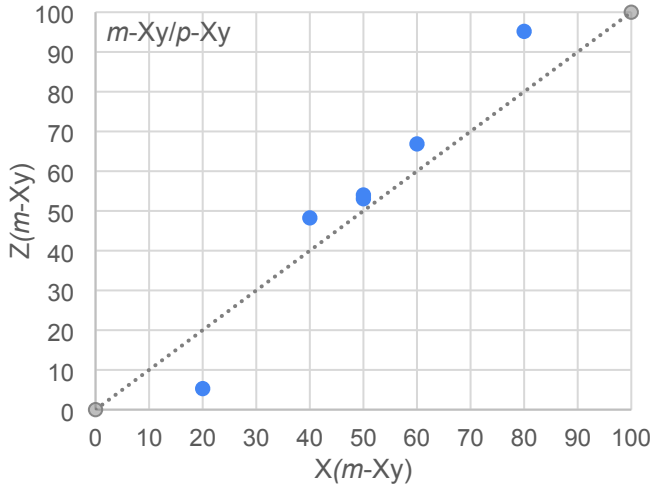

e)

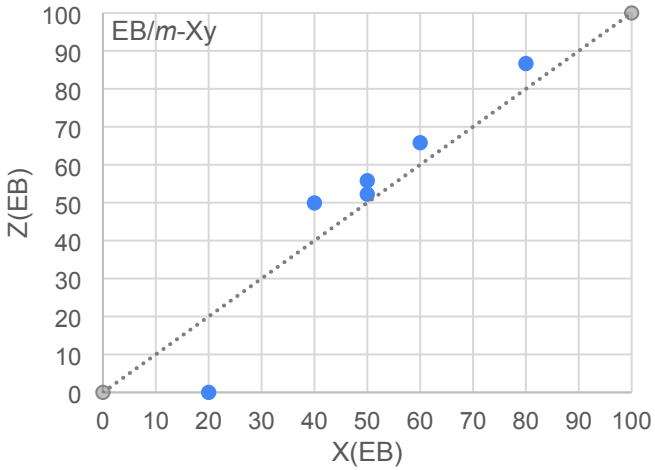

f)

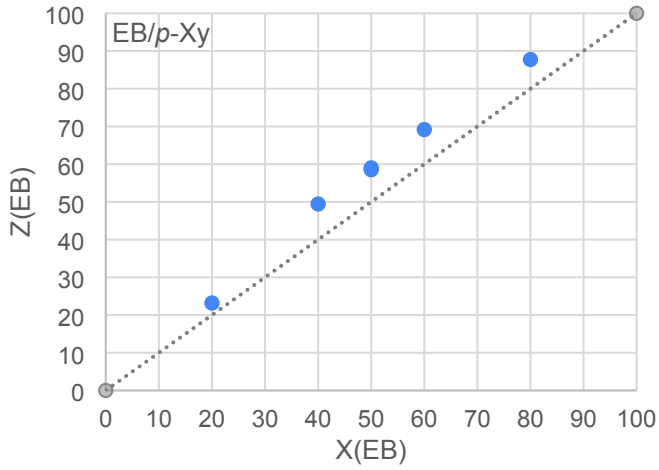

Figure 2 Selectivity profiles for the binary guest competition experiments involving a) *o*-Xy/*m*-Xy, b) *o*-Xy/*p*-Xy, c) *o*-Xy/EB, d) *m*-Xy/*p*-Xy, e) EB/*m*-Xy and f) EB/*p*-Xy.

View Article Online
DOI: 10.1039/D6CE00160B

Figures 2a and f demonstrate that in the *o*-Xy/*m*-Xy and EB/*p*-Xy binary solutions, **H** was selective for only one guest across the concentration range, namely *o*-Xy and EB, respectively. On the other hand, Figures 2b–e reveal that the preferential behaviour of **H** was guest concentration dependent. In each of these instances, the host compound in the 20/80 mixtures selected more of the guest present in the higher concentration. Therefore, the complexes emanating from the 20/80 *o*-Xy/*p*-Xy, *o*-Xy/EB, *m*-Xy/*p*-Xy and EB/*m*-Xy solutions were enriched in *p*-Xy, EB, *p*-Xy and *m*-Xy, correspondingly. All of the remaining data points in these four plots, however, showed a consistent host preference for the alternative guest solvent, those listed first in these guest pairs.

From Table 3, K was too low (1.1–8.8) in most instances to suggest that **H** would be an ideal host candidate for these separations through host-guest chemistry. Strikingly, though, two selectivity coefficients were calculated to be infinite as a result of the fact that only one guest species was observed in the so formed complexes. The applicable inclusion compounds were those obtained from the 20/80 *o*-Xy/EB and 20/80 EB/*m*-Xy solutions in which only EB and *m*-Xy, respectively, were detected in the crystals. These results indicate that **H** may behave as a purification tool for solvents EB and *m*-Xy that are tainted with, in turn, small quantities of *o*-Xy and EB.

Table 3 Selectivity coefficients for the data points contained in the selectivity profiles.

	K Values					
Binary Mixture	20:80	40:60	50:50[a]	50:50[a]	60:40	80:20
o-Xy/*m*-Xy	1.8 (*o*-Xy)	1.3 (*o*-Xy)	1.4 (*o*-Xy)	1.6 (*o*-Xy)	1.9 (*o*-Xy)	2.4 (*o*-Xy)
o-Xy/*p*-Xy	8.8 (*p*-Xy)	1.8 (*o*-Xy	6.4 (*o*-Xy)	6.7 (*o*-Xy)	5.5 (*o*-Xy)	6.3 (*o*-Xy)
o-Xy/EB	**∞ (EB)**	1.5 (*o*-Xy)	4.3 (*o*-Xy)	4.0 (*o*-Xy)	5.5 (*o*-Xy)	5.2 (*o*-Xy)
m-Xy/*p*-Xy	4.5 (*p*-Xy)	1.4 (*m*-Xy)	1.1 (*m*-Xy)	1.2 (*m*-Xy)	1.4 (*m*-Xy)	4.9 (*m*-Xy)
EB/*m*-Xy	**∞ (*m*-Xy)**	1.5 (EB)	1.3 (EB)	1.1 (EB)	1.3 (EB)	1.6 (EB)
EB/*p*-Xy	1.2 (EB)	1.5 (EB)	1.4 (EB)	1.4 (EB)	1.5 (EB)	1.8 (EB)

[a]In all cases, the 50:50 experiments were conducted in duplicate (see Section 3.2).

3.4 Single crystal X-ray diffractometry

Single crystal X-ray diffraction (SCXRD) experiments were performed on each of the three complexes prepared in this investigation (**H**·*o*-Xy, **H**·*m*-Xy **H**·2(*p*-Xy)) in addition to guest-free **H**, which was obtained after crystallization from EB. The applicable crystallographic data for these experiments are contained in Table 4. Apohost compound **H** and its *p*-xylene inclusion compound crystallized in the triclinic crystal system and space group *P*–1, while both **H**·*o*-Xy and **H**·*m*-Xy crystallized in the monoclinic crystal system and, in both cases, the space group was $P2_1/n$. In fact, upon a closer inspection of the unit cell parameters of these two complexes, it was clear that the host packing in each one was isostructural.

In **H**·*o*-Xy, the guest was disordered over two positions (with site occupancy factors (s.o.f.s) of 0.665(5) and 0.335(5)), while the crystals of the **H**·*m*-Xy inclusion compound were flexible, flat rods that were weakly diffracting, resulting in a high R value (0.1031). Additionally, one of the two guest molecules in the unit cell of **H**·2(*p*-Xy) also possessed positional disorder (s.o.f.s 0.749(7) and 0.251(7)), while the other guest species was not disordered.

The unit cells for guest-free **H** (Figure 3a, top, a stereoview) and the **H**·*o*-Xy, (Figure 3b, representing also isostructural **H**·*m*-Xy) and **H**·2(*p*-Xy) (Figure 3c) complexes are also provided here. The host molecules in the crystals of each of guest-free **H** (Figure 3a, bottom, also a stereoview) and **H**·2(*p*-Xy) (Figure 3c) possessed an inversion of symmetry and, consequently, the two NH groups of the linker units were positioned in an antiperiplanar orientation (180.00°) with respect to one another. However, these molecules in the **H**·*o*-Xy and **H**·*m*-Xy complexes (which demonstrated an isostructural host packing motif) had these NH moieties in a more gauche orientation (66.61 and 66.08°). Moreover, after guest removal from the packing calculations and an analysis of the resulting spaces by means of a probe with a 1.2 Å radius, it was possible to prepare the void diagrams as demonstrated on the right-hand side in Figures 3b and c. In all of these complexes, guests were accommodated in endless channels, unidirectional in the case of **H**·*o*-Xy and **H**·*m*-Xy (Figure 3b) and bidirectional in the complex with *p*-xylene (Figure 3c, with the disordered guest species in a different channel to the ordered guest molecules).

View Article Online
DOI: 10.1039/D6CE00160B

Table 4 Crystallographic data for guest-free **H** and its complexes with *o*-Xy, *m*-Xy and *p*-Xy.

	H	**H**·*o*-Xy	**H**·*m*-Xy	**H**·2(*p*-Xy)
Chemical formula	$C_{42}H_{36}N_2O_4$	$C_{42}H_{36}N_2O_4$, C_8H_{10}	$C_{42}H_{36}N_2O_4$, C_8H_{10}	$C_{42}H_{36}N_2O_4$, 2(C_8H_{10})
Formula weight	632.73	738.89	738.89	845.04
Crystal system	Triclinic	Monoclinic	Monoclinic	Triclinic
Space group	*P*–1	$P2_1/n$	$P2_1/n$	*P*–1
μ (Mo-Kα)/mm^{-1}	0.084	0.078	0.080	0.075
a/Å	11.8593(4)	17.8696(12)	18.206(3)	8.6383(3)
b/Å	15.2353(6)	10.5775(7)	10.4572(14)	9.2258(3)
c/Å	16.0329(6)	22.5364(14)	21.564(3)	15.8317(5)
alpha/°	64.5256(12)	90	90	104.060(1)
beta/°	81.2254(12)	111.015(2)	109.528(5)	91.052(1)
gamma/°	67.5368(12)	90	90	108.317(1)
V/Å^3	2416.52(16)	3976.4(5)	3869.3(10)	1155.74(7)
Z	3	4	4	1
F(000)	1002	1568	1568	450
Temp./K	200	200	200	200
Restraints	0	222	0	60
N_{ref}	9820	8078	5663	5731
N_{par}	665	557	426	335
R	0.0533	0.0760	0.1031	0.0545
wR2	0.1163	0.1356	0.1802	0.1252
S	1.13	1.21	1.11	1.11
θ min–max/°	2.0, 26.4	2.2, 26.5	2.2, 23.5	2.4, 28.3
Tot. data	109441	137242	64336	100762
Unique data	9820	8078	5663	5731
Observed data [I > 2.0 sigma(I)]	8370	6436	3882	4256
R_{int}	0.058	0.106	0.183	0.045
Completeness	0.997	0.998	0.991	0.998
Min. resd. dens./e/Å^3	–0.22	–0.33	–0.36	–0.26
Max. resd. dens./e/Å^3	0.31	0.35	0.37	0.30
Density/g·cm^{-3}	1.304	1.234	1.268	1.214

a)

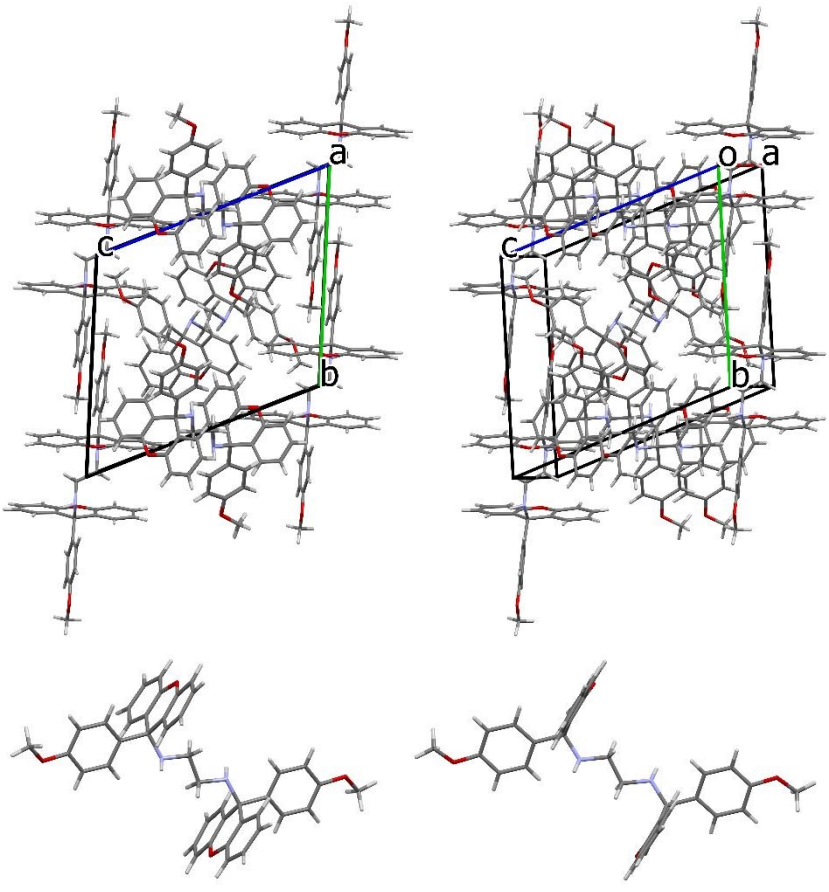

View Article Online
DOI: 10.1039/D6CE00160B

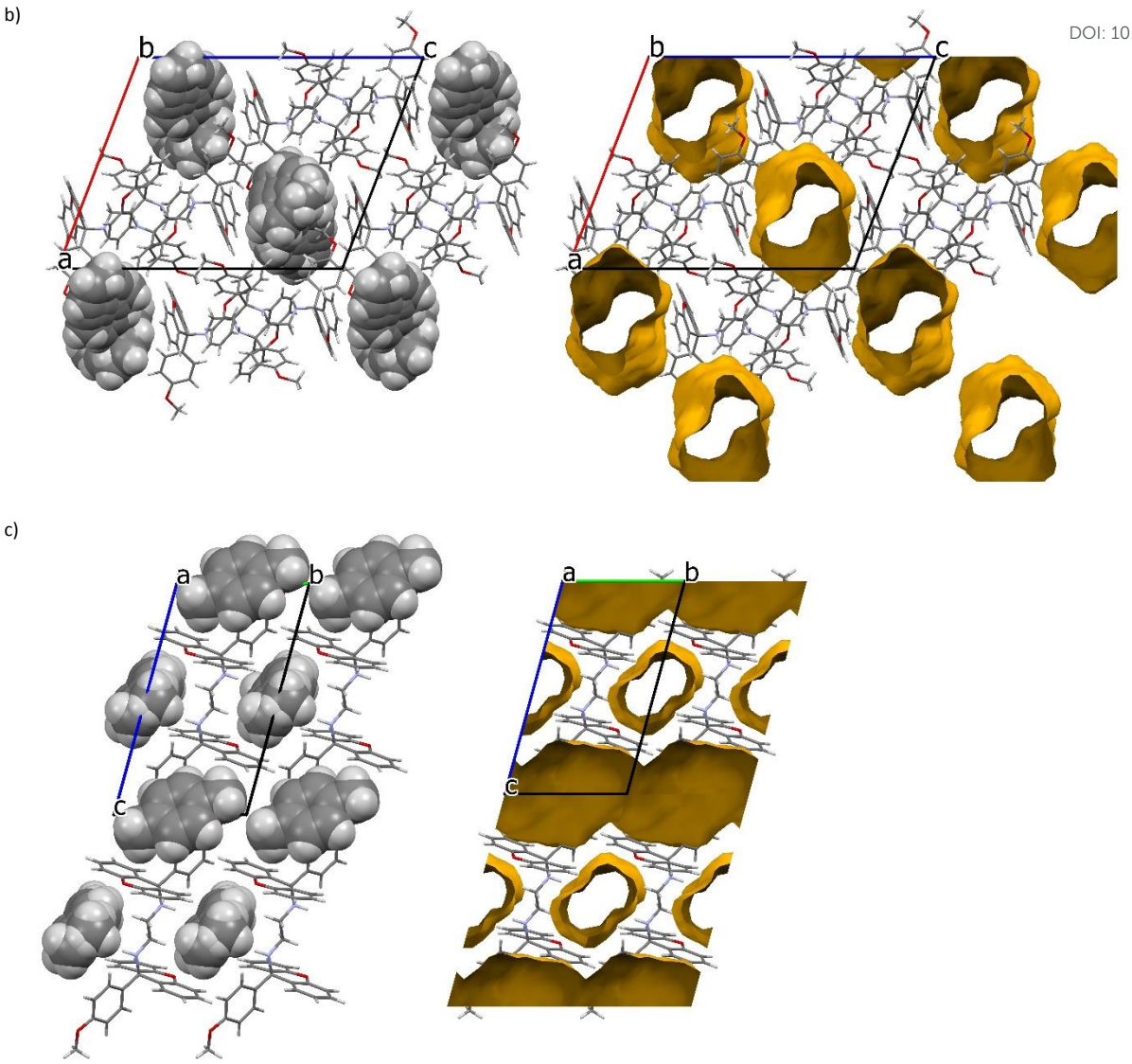

Figure 3 Unit cells for a) guest-free **H** (top, stereoview) (and the host molecular geometry (bottom, stereoview)), b) **H**·*o*-Xy (representing also **H**·*m*-Xy) and c) **H**·2(*p*-Xy); the void diagrams are provided on the right-hand side in b) and c).

The close contacts that stabilized these crystalline forms were subsequently investigated. The packing of guest-free **H** did not involve any significant π···π interactions; however, two C–H···π contacts were identified in the unit cell, with H···π distances of 2.93 and 2.68 Å (C···π, 3.687(3) and 3.587(2) Å, 138 and 161°). Additionally, three nonclassical intermolecular hydrogen bonds of the C–H···O type were observed, involving the aromatic, methoxy or linker hydrogen atoms interacting with the oxygen atoms of the central xanthenyl B-ring or the methoxy moiety. These distances measured between 2.55 and 2.69 Å (H···O) and the applicable angles were 145–151°. Figure 4 (left) is an illustrative example, involving two methoxy moieties ((MeO)C–H···O–C(MeO), 2.55 Å, 148°). Finally, in these crystals was also noted a classical intermolecular hydrogen bond (Figure 4, right): the amino hydrogen atom of the linker unit experienced a stabilizing close contact with the oxygen atom of a *para*–methoxy group of a neighbouring molecule with measurements 2.52(2) Å (H···O), 3.373(2) Å (N···O) and 155.9(18)°.

View Article Online
DOI: 10.1039/D6CE00160B

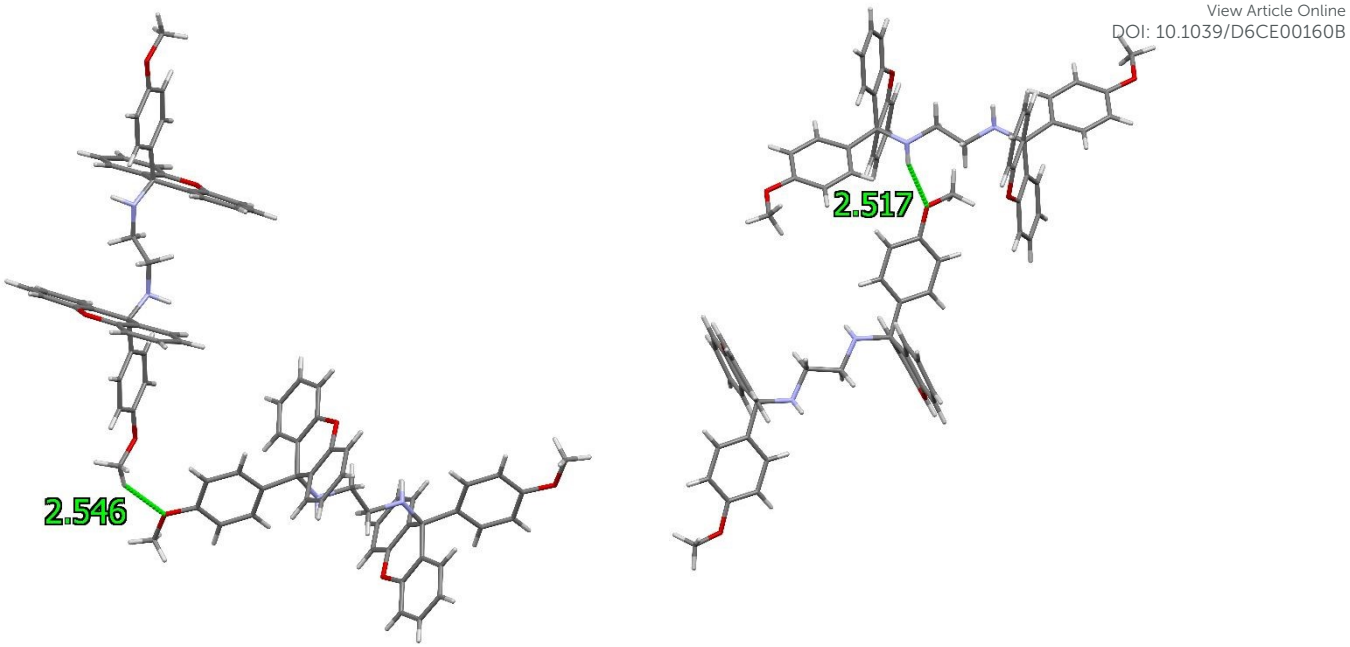

Figure 4 Examples of nonclassical (left) and classical (right) intermolecular hydrogen bonds in the unit cell of guest-free **H**.

As in guest-free **H**, no π···π close contacts were evident in the complex containing *o*-Xy. However, and again, C–H···π interactions were observed, both between host molecules (2.80–2.96 Å, 3.736(3)–3.807(3) Å, 149–168°) and between host and guest species, numbering two in the latter instance (Figure 5), involving both disorder guest components, where the guest molecules served as the proton donors; here, measurements were 2.77 Å, 3.605(4) Å, 148° and 2.67 Å, 3.554(9), 155°. (The guest disorder over two positions is also clearly demonstrated in this figure.) Moreover, the only classical hydrogen bonding in this complex was intramolecular in nature, serving to stabilise the geometry of each host molecule, between the hydrogen atom of the amino group of the linker unit and the second nitrogen atom of the same unit (2.61 Å (H···N), 2.945(3) Å (N···N) and 104°), while both intra- (C–H···N, 2.38 Å, 2.764(3) Å, 103° and 2.45 Å, 2.804(3), 102°) and intermolecular (C–H···O, 2.57 Å, 3.375(3) Å, 143°) nonclassical hydrogen bonds involving molecules of **H** were also identified.

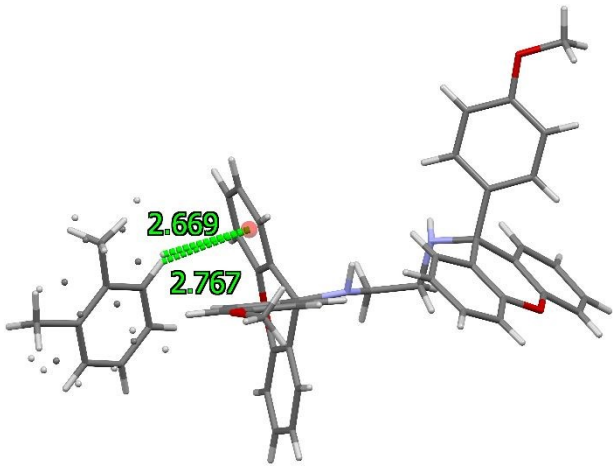

Figure 5 The (guest)C–H···π(host) close contacts in **H**·*o*-Xy, involving both guest disorder orientations.

Many similarities were noted in the noncovalent interactions present in **H**·*o*-Xy and **H**·*m*-Xy, expectedly, given the isostructural nature of their host packing. These include (host)C–H···π(host) (2.97–2.98 Å, 3.747(3)–3.899(3) Å, 138–166°) contacts as well as one (guest)C–H···π(host) (2.93 Å, 3.815(4) Å, 155°) intermolecular interaction. Once more, the conformation of the host molecule was stabilized by means of a singular intramolecular classical hydrogen bond involving the linker unit amino moieties

View Article Online
DOI: 10.1039/D6CE00160B

(N–H···N, 2.55 Å, 2.914(5) Å, 106°), while the nonclassical hydrogen bonds were of the C–H···N (2.42 Å, 2.771(5) Å, 101° and 2.34 Å, 2.715(5) Å, 103°) and C–H···O (2.52 Å, 3.331(5) Å, 143°) types, as was the case in the *o*-Xy-containing inclusion complex.

In the case of **H**·2(*p*-Xy), which also did not experience any π···π contacts, was identified an intermolecular (host)C–H···π(host) (2.96 Å, 3.692(2) Å, 133°) interaction involving a proton of the methoxyl moiety and an aromatic ring of the xanthenyl system. Furthermore, as was the occasion in the complexes with *o*-Xy and *m*-Xy, contacts of this type were also observed between host and guest species where the guest molecule was the proton donor; two such contacts were evident, measuring 2.96 Å, 3.710(7) Å, 133° and 2.67 Å, 3.582(17) Å, 161°, and involving only the two components of the disordered guest molecule and not the other non-disordered guest species, as illustrated clearly in Figure 6. In fact, the ordered guest molecule was held in the crystals of the complex by means of steric factors only and no short contacts with the host species could be identified. Finally, the host molecule in this complex was not stabilized by an intramolecular classical N–H···N hydrogen bond, in contrast with this species in **H**·*o*-Xy and **H**·*m*-Xy. However, a singular intramolecular host C–H···N nonclassical bond of this type was identified (2.42 Å, 2.788(2) Å, 103°).

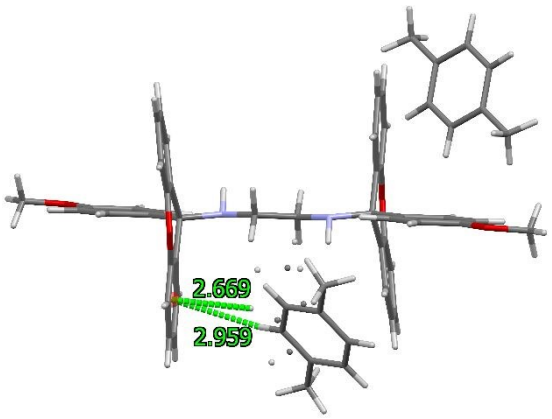

Figure 6 The (guest)C–H···π(host) contacts involving only the two components of the disordered guest molecule and not the ordered guest species.

Interestingly, these SCXRD data provide some insight into the selectivity behaviour of **H** during crystallization experiments from mixed guest solutions: all of the guest molecules in **H**·*o*-Xy and **H**·*m*-Xy, having guests that were more preferred, were retained in their channels through C–H···π contacts with the host compound, while not all of the *p*-Xy molecules (*p*-Xy being distinctly disfavoured by **H**) experienced this type of interaction (only the two disordered guest components were retained in this manner, and not the ordered guest molecules). Furthermore, the nature of the guest accommodation was also distinctly different: preferred *o*-Xy and *m*-Xy occupied unidirectional channels, while *p*-Xy was located in two channels in two separate orientations in its complex, one housing the ordered and the other the disordered guest molecules.

3.5 Thermal analysis

Figures 7a–c depict the overlaid thermogravimetric (TG, red), its derivative (DTG, green) and differential scanning calorimetric (DSC, blue, endo up) for the thermal experiments conducted on each of **H**·*o*-Xy, **H**·*m*-Xy and **H**·2(*p*-Xy), while the more applicable thermal data from these traces are summarised in Table 5.

Table 5 Thermal data for the inclusion compounds of **H** with the xylene isomers.

Complex	T_{on}[a] (°C)	Mass loss (%) (expected)	Mass loss (%) (experimental)
H·*o*-Xy	41.7	14.4	13.6
H·*p*-Xy	39.2	14.4	15.4
H·2(*p*-Xy)	41.3	25.1	25.2

[a]T_{on} is the onset temperature for the guest release event and was estimated from the DTG trace in each case.

Each of the guest species in the three complexes was released in a distinct single-stepped process (Figures 7a–c). Furthermore, the onset temperatures for this guest release event (T_{on}) in each of the three experiments were extremely comparable (41.7, 39.2 and 41.3 °C for **H**·*o*-Xy, **H**·*m*-Xy and **H**·2(*p*-Xy), respectively), suggesting that these inclusion compounds possess very similar relative thermal stabilities. This observation is not entirely surprising in the case of **H**·*o*-Xy and **H**·*m*-Xy since these

View Article Online
DOI: 10.1039/D6CE00160B

complexes shared a host packing. These thermal data do not, as a result, provide a rationalization for the selectivity behaviour of **H** when presented with guest mixtures in that the more preferred guests did not form the more stable complexes, according to these data. However, as stipulated earlier, such explanations were clarified through the SCXRD experiments.

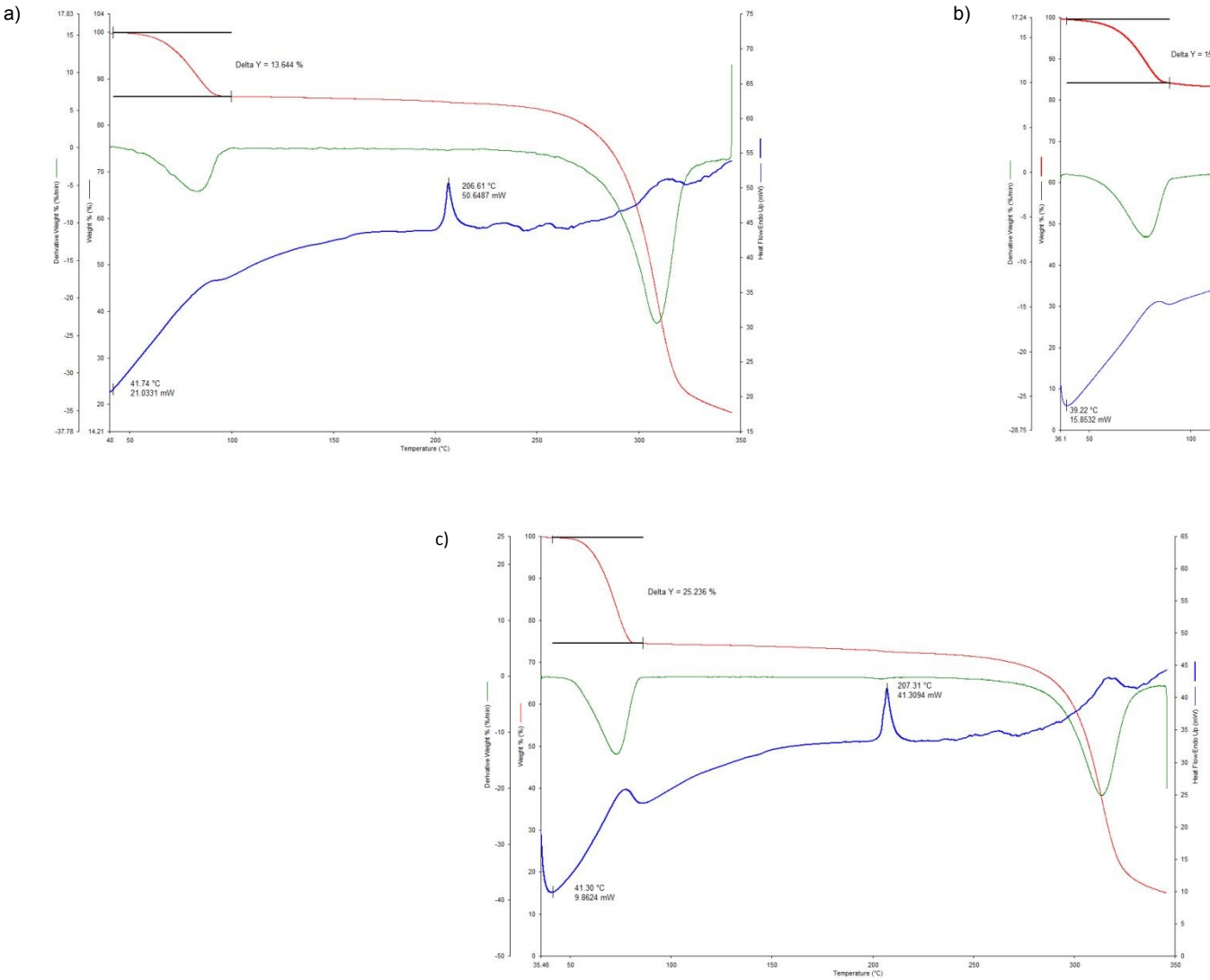

Figure 7 Overlaid TG (red), DTG (green) and DSC (blue, endo up) traces for the inclusion complexes with a) **H**·*o*-Xy, b) **H**·*m*-Xy and c) **H**·2(*p*-Xy).

View Article Online
DOI: 10.1039/D6CE00160B

4. Conclusions

In the present investigation, the host compound *N*,*N'*-bis(9-(4-methoxyphenyl)-9*H*-xanthen-9-yl)ethane-1,2-diamine (**H**) was demonstrated to possess inclusion ability for *o*-Xy, *m*-Xy and *p*-Xy, while EB was not enclathrated in analogous experimental conditions and only apohost **H** was isolated in this particular instance. The H:G ratios of the three successfully furnished complexes were 1:1, 1:1 and 1:2 (*o*-Xy, *m*-Xy and *p*-Xy). When **H** was crystallized from guest solutions, a host selectivity order of *o*-Xy > EB > *m*-Xy > *p*-Xy was noted. In fact, it was shown that **H** may serve to purify EB and *m*-Xy solvents when contaminated with small quantities of *o*-Xy and EB, respectively. SCXRD experiments demonstrated that more preferred *o*-Xy and *m*-Xy always experienced a (guest)C–H···π(host) close contact with **H**, facilitating guest retention, while not all of the guest molecules in **H**·2(*p*-Xy) were involved in these types of stabilizing interactions with the host species, thus explaining the low preference of **H** for *p*-Xy. The relative thermal stabilities of the three single solvent complexes were, moreover, established to be equivalent through thermoanalytical experiments since T_{on}, the onset temperatures of the guest release events, ranged between only 39.2 and 41.7 °C.

Supplementary information

The crystal structures of guest-free **H**, **H**·*o*-Xy, **H**·*m*-Xy and **H**·2(*p*-Xy) were deposited at the Cambridge Crystallographic Data Centre and their respective CCDC numbers are 2530251–2530254. Crystallographic data for these structures are freely accessible at www.ccdc.cam.ac.uk/structures/. The relevant ORTEP diagrams and ^{1}H-NMR spectra may also be found in this section.

Author contributions

B.B.: conceptualization; methodology; funding acquisition; project administration; resources; supervision; visualization; writing the original draft. M.A.: investigation; methodology; validation; assisting with original draft. E.C.H.: data curation; formal analysis.

Conflict of interest

There are no conflicts of interest to declare.

Acknowledgements

Financial support is acknowledged from the Nelson Mandela University and the National Research Foundation (NRF) of South Africa.

References

1. J. Fabri, U. Graeser, T. A. Simo (2000), Xylenes, in: *Ullmann's Encyclopedia of Industrial Chemistry*, Wiley-VCH Verlag GmbH & Co. KGaA, Weinheim, Germany. 10.1002/14356007.a28_433

2. W. J. Cannella (2000), Xylenes and ethylbenzene, in: *Kirk-Othmer Encyclopedia of Chemical Technology*, John Wiley & Sons, New York. 10.1002/0471238961.2425120503011414.a01

3. L. Berg, Separation of ethylbenzene from *p*- and *m*-xylene by extractive distillation using mixtures of oxygenated organic compounds, *AIChE J.*, 1983, **29**, 694–696.

4. L. Berg, Separation of ethyl benzene from xylenes by azeotropic distillation, United States Patent, 5,417,812, 1995.

5. Q. Shi, J. C. Gonçalves, A. F. P. Ferreira, A. E. Rodrigues, A review of advances in production and separation of xylene isomers, *Chem. Eng. Process. Process Intensif.*, 2021, **169**, 108603.

6. G. Zhang, Y. Ding, A. Hashem, A. Fakim, N. M. Khashab, Xylene isomer separations by intrinsically porous molecular materials, *Cell Rep. Phys. Sci.*, 2021, **2**, 100470.

7. D. Han, S. Wu, Z. Xia, R. Ao, L. Oi, Review: Advances in efficient separation of paraxylene from mixed xylene isomers using SMB technology and MOF materials, *J. Ind. Eng. Chem.*, 2025, **148**, 52–68.

8. M. Khosravi, M. Jafari, K. Ghasemzadeh, A. Iulianelli, Enhancing styrene production: CFD analysis of a Pd-based membrane reactor to carry out ethylbenzene dehydrogenation, *Fuel Process. Technol.*, 2025, **270**, 108191.

9. D. Royuela, A. Veses, T. García, R. Murillo, J. D. Martínez, Advances in the circular economy of polystyrene: A critical review of pyrolysis in pilot-scale systems, distillation, and re-polymerization, *J. Environ. Chem. Eng.*, 2026, **14**, 121633.

10. Y. Takai, T. Mizutani, M. Leda, Comparative study on the electronic properties of *p*-xylene polymers prepared by plasma-polymerization and vapor phase pyrolysis, *Jpn. J. Appl. Phys.*, 1987, **26**, 812–817.

11. L. A. Errede, R. S. Gregorian, J. M. Hoyt, The chemistry of xylylenes. VI. The polymerization of *p*-xylylene, *J. Am. Chem. Soc.*, 1960, **82**, 5218–5223.

12. L. Alexandrova, R. Salcedo, Pathway for polymerization of *p*-xylylenes, *Polym.*, 1994, **35**, 4656–4658.

13. A. Akbari, S. M. Alavi, The effect of cesium and antimony promoters on the performance of Ti-phosphate-supported vanadium(V) oxide catalysts in selective oxidation of *o*-xylene to phthalic anhydride, *Chem. Eng. Res. Des.*, 2015, **102**, 286–296.

14. P. Eversfield, T. Lange, M. Hunger, E. Klemm, Seelective oxidation of *o*-xylene to phthalic anhydride on tungsten, tin, and potassium promoted VO_x on TiO_2 monolayer catalysts, *Catal. Today*, 2019, **333**, 120–126.

15. A. G. Dixon, Y. Wu, Partial oxidation of *o*-xylene to phthalic anhydride in a fixed bed reactor with axial thermowells, *Chem. Eng. Res. Des.*, 2020, **159**, 125–137.

16. X. -Li. Long, Z. -H. Wang, S. -Q. Wu, S. -M. Wu, H. -F. Lv, W. -K. Yuan, Production of isophthalic acid from m-xylene oxidation under the catalysis of the H3PW12O40/carbon and cobalt catalytic system, *J. Ind. Eng. Chem.*, 2014, **20**, 100–107.

17. H. -F. Lv, S. -Q. Wu, N. Liu, X. -L. Long, W. -K. Yuan, A study on the *m*-xylene oxidation to isophthalic acid under the catalysis of bromine-free homogeneous catalytic system, *Chem. Eng. J.*, 2011, **172**, 1045–1053.

18. C. H. Seo, Y. H. Kim, Separation of ethylbenzene and *p*-xylene using extractive distillation with *p*-dinitrobenzene, *Sep. Purif. Technol.*, 2019, **209**, 1–5.

19. G. -C. Lin, C. A. Chang, Heavy alkylated benzene stationary phase for the gas-liquid chromatographic separation of ethylbenzene, xylenes, styre, iso- and *n*-propylbenzene, *J. Chromatogr. A*, 1987, **409**, 371–376.

20. G. Zhang, S. Xu, X. Zeng, Y. Jiang, R. Zhou, Z. Lai, Advances in inorganic membranes for xylene isomers separation: Fabrication strategies and mechanistic insights, *Chin. J. Chem. Eng.*, 2025, https://doi.org/10.1016/j.cjche.2025.11.011.

21. M. Rasouli, N. Yaghobi, S. Z. M. Gilani, H. Atashi, M. Rasouli, Influence of monovalent alkaline metal cations on binder-free nano-zeolite X in *para*-xylene separation, *Chin. J. Chem. Eng.*, 2015, **23**, 64–70.

22. Y. Liu, C. Wang, Q. Yang, Q. Ren, Z. Bao, Separation of xylene isomers using metal-organic frameworks: Addressing challenges in the petrochemical industry, *Coord. Chem. Rev.*, 2025, **523**, 216229.

23. W. Wang, Y. Zhang, B. Tang, H. Hou, S. Tang, A. Luo, Chiral hydrogen-bonded organic frameworks used as a chiral stationary phase for chiral separation in gas chromatography, *J. Chromatogr. A*, 2022, **1675**, 463150.

24. L. Li, L. Guo, D. H. Olson, S. Xian, Z. Zhang, Q. Yang, K. Wu, Y. Yang, Z. Bao, Q. Ren, J. Li, Discrimination of xylene isomers in a stacked coordination polymer, *Science*, 2022, **377**, 335–339.

25. J. -M. Lehn, *Supramolecular Chemistry Concepts and Perspectives*, VCH Verlagsgesellschaft mbH, Weinheim (Bundesrepublik Deutschland), 1st edn., 1995.

26. J. W. Steed, J. L. Atwood, *Supramolecular Chemistry*, Wiley, 3rd edn., 2022.

27. B. Barnardo, B. Barton, M. R. Caira, E. C. Hosten, Evaluation of the behaviour of two tricyclic-fused host systems in the presence of single and mixed isomers of the C_8H_{10} aromatic crude oil fraction, *Cryst. Growth Des.,* 2024, **24**, 5603–5613.

28. B. Barton, M. R. Caira, L. de Jager, E. C. Hosten, *N*,*N*′-Bis(9-phenyl-9-thioxanthenyl)ethylenediamine: highly selective host behavior in the presence of xylene and ethylbenzene guest mixtures, *Crys. Growth Des.*, 2017, **17**, 6660–6667.

29. B. Barton, D. V. Jooste, E. C. Hosten, Synthesis and assessment of compounds *trans*-*N*,*N*′-bis(9-phenyl-9-xanthenyl)cyclohexane-1,4-diamine and *trans*-*N*,*N*′-bis(9-phenyl-9-thioxanthenyl)cyclohexane-1,4-diamine as hosts for potential xylene and ethylbenzene guests, *J. Incl. Phenom. Macrocycl. Chem.*, 2019, **93**, 333–346.

30. B. Barton, U. Senekal and E. C. Hosten, Compounds *N*,*N*′-bis(9-cyclohexyl-9-xanthenyl)ethylenediamine and its thio derivative, *N*,*N*′-bis(9-cyclohexyl-9-thioxanthenyl)ethylenediamine, as potential hosts in the presence of xylenes and ethylbenzene: Conformational analyses and molecular modelling considerations, *Tetrahedron*, 2019, **75**, 3399–3412.

31. B. Barton, D. V. Jooste, E. C. Hosten, Behaviour of host compounds 1,2-DAX and 1,2-DAT in the presence of mixed xylene and ethylbenzene guest solvents, and comparisons with their 1,4 host derivatives, *J. Incl. Phenom. Macrocycl. Chem.*, 2021, **100**, 155–167.

32. B. Barton, D. B. Trollip, E. C. Hosten, Selected tricyclic fused systems: Host behaviour in the presence of mixed xylenes and ethylbenzene, *Cryst. Growth Des.*, 2022, **22**, 6726–6734.

33. B. Barton, E. C. Hosten, P. L. Pohl, Discrimination between *o*-xylene, *m*-xylene, *p*-xylene and ethylbenzene by host compound (*R*,*R*)-(−)-2,3-dimethoxy-1,1,4,4-tetraphenylbutane-1,4-diol, *Tetrahedron*, 2016, **72**, 8099–8105

34. B. Barton, U. Senekal, E. C. Hosten, Comparing the host behaviour of roof-shaped compounds *trans*-9,10-dihydro-9,10-ethanoanthracene-11,12-dicarboxylic acid and its dimethyl ester in the presence of mixtures of xylene and ethylbenzene guests, *CrystEngComm*, 2021, **23**, 4560–4572.

35. B. Barton, B. Barnardo and E. C. Hosten, Selectivity behaviour of two roof-shaped host compounds in the presence of xylene and ethylbenzene guest mixtures, *CrystEngComm*, 2021, **23**, 7278–7288.

36. Bruker (2012). APEX5, SAINT. Bruker AXS Inc., Madison, Wisconsin, USA.

37. L. Krause, R. Herbst-Irmer, G. M. Sheldrick and D. Stalke, Comparison of silver and molybdenum microfocus X-ray sources for single-crystal structure determination, *J. Appl. Cryst.*, 2015, **48**, 3–10.

38. G. M. Sheldrick, SHELXT – Integrated space-group and crystal structure determination, *Acta Cryst.*, 2015, A**71**, 3–8.

39. G. M. Sheldrick. Crystal structure refinement with SHELXL, *Acta Cryst.*, 2015, C**71**, 3–8.

40. C. B. Hübschle, G. M. Sheldrick and B. Dittrich. ShelXle: a Qt graphical user interface for SHELXL, *J. Appl. Cryst.*, 2011, **44**, 1281–1284.

41. L. J. Farrugia. WinGX and ORTEP for Windows: An update, *J. Appl. Cryst.*, 2012, **45,** 849–854.

42. B. Barton, Host-guest chemistry: The synthesis and assessment of host compounds based on the 9-arylxanthenyl and related systems, PhD Thesis, University of Port Elizabeth, Port Elizabeth, 1996.

43. A. M. Pivovar, K. T. Holman, M. D. Ward, Shape-selective separation of molecular isomers with tuneable hydrogen-bonded host frameworks, *Chem. Mater.*, 2001, **13**, 3018–3031.

44. N. M. Sykes, H. Su, E. Weber, S. A. Bourne, L. R. Nassimbeni, Selective enclathration of methyl- and dimethylpiperidines by fluorenol hosts. *Cryst. Growth Des.* 2017, **17**, 819–826.

45. C. Macrae, I. Sovago, S. Cottrell, P. Galek, P. McCabe, E. Padcock, M. Platings, G. Shields, J. Stevens, M. Towler, P. Wood, Mercury 4.0: From visualization to analysis. Design and prediction, *J. Appl. Crystallogr.*, 2020, **53**, 226–235.

DATA AVAILABILITY STATEMENT

View Article Online
DOI: 10.1039/D6CE00160B

The crystal structures of guest-free **H**, **H**·*o*-Xy, **H**·*m*-Xy and **H**·2(*p*-Xy) were deposited at the Cambridge Crystallographic Data Centre and their respective CCDC numbers are 2530251–2530254. These data may be obtained free of charge at www.ccdc.cam.ac.uk/data_request/cif.